

## **Effect of steel slag and Portland cement in the rate of hydration and strength of blast furnace slag pastes**

Juan Lizarazo-Marriaga<sup>a,b</sup>, Peter Claisse<sup>b</sup>, Eshmaiel Ganjian<sup>b</sup>

<sup>a</sup> Departamento de Ingeniería Civil, Universidad Nacional, Bogotá, Colombia.

<sup>b</sup> Construction Materials Applied Research Group, Coventry University CV1 5FB, UK.

### **Abstract**

This paper presents an experimental study of the influence of Steel Basic Oxygen Slag (BOS) and Portland cement (OPC) on the compressive strength and the hydration mechanisms of blended Grounded Granulated Blast Furnace Slag (GGBS) pastes. The compressive strength, the mineralogical changes due to hydration, the setting times, the alkalinity of the raw materials and the pore solution, and the volume stability were measured on binary and ternary mixes. It is concluded that the steel slag can be used as an activator of GGBS and the optimum composition of those materials was determined with a proposed parameter called “slag index”. The properties measured in blended OPC-GGBS-BOS mixes showed encouraging results to be used industrially. The mechanisms of hydration of the blended slag mixes are discussed and a hydration model of the blended system GGBS-BOS is proposed.

### **1. Introduction**

Slag is a by-product of the metallurgical industry where metals such as iron, copper, lead, or aluminium, are purified or transformed. Depending on its chemical and physical properties the slag can be used in the construction industry as aggregate in granular bases, asphalt mixes, and concrete mixes; as cement replacement, or in embankments or fill applications. Worldwide the most commonly used slag is Granulated Blast Furnace slag (GGBS), however, efforts are being made to use other types of slag that are available in large quantities and, in the same way as GGBS, could have some potential cementitious properties.

GGBS slag is a non metallic material resulting from the combination of the calcium and magnesium in calcareous stones with the aluminates and silicates in iron ore. The chemical and mineralogical composition of GGBS depends on the characteristics of the metallurgical process and materials; however, the principal compounds are CaO, SiO, Al<sub>2</sub>O, and MgO that are present in most hydraulic binders. Compared to OPC, slag has a higher silica content and lower calcium content, and contains low quantities of ferric oxide. For a typical sample of GGBS the glass content is around 85-90%, and with this, the basicity is considered the factor governing its hydraulicity. The more basic the slag, the greater its hydraulic reactivity in the presence of alkaline activators (Detwiler et al. 1996). According to Tailing and Krivenko (1997), the hydration of slag involves complex chemical and physical reactions such as adsorption, ion exchange, dissolution, and hydrolysis. When contact with water, the slag grains develop some external insoluble thin layers composed of silica and an alkali earth hydrosilicate preventing further reactions on their surface. Under highly alkali environments, the formation of this external film is inhibited and no retardation of the hydration process occurs.

GGBS as a binder can be used in different ways. Blended cements of GGBS and ordinary Portland cement (OPC) have been used for more than 100 years and are covered by international standards (ASTM-C595 2008). The combination of GGBS with OPC and pozzolans is reported by the American Concrete Institute committee 233 (ACI-233 2003). GGBS-alkali activated binder systems are used extensively in Eastern Europe (Tailing and Krivenko 1997), and the activation of slags with sulphate minerals have been used for more than 50 years in Europe (Matschei et al. 2005).

Steel slag is a by-product of the transformation of iron to steel. Pig iron is collected from the blast furnace, transferred to the steel plant and charged into a steelmaking vessel, typically a basic oxygen furnace (BOF). During the conversion, pig iron and scrap are melted and fluxes of lime or dolomite are mixed into the furnace. In order to take out the impurities of the melting steel, high pressure oxygen is injected removing undesirable contaminants, which are combined with the lime or dolomite to produce the Basic Oxygen Steel (BOS)\_slag. After refining, the liquid steel is poured into a ladle to continue the metallurgical process, while the slag is collected with other processes.

Steel slag has not been extensively used as a cement replacement because theoretically it has some disadvantages:

- A highly variable mineralogical composition.
- The low content of reactive calcium silicate compounds gives to the steel slag poor cementing properties.
- The high content of free calcium and magnesium oxides cause volume expansion problems.
- Steel slag has higher density than other binders.
- The possibility of leaching of metals such as chromium and molybdenum has been an environmental obstacle.

Despite the problems associated with steel slag, it has many possibilities for use in the cement and concrete industry. In China, for example, it has been commercialized for long time in a cement that contains 35% Portland clinker, 5% gypsum, 30% steel furnace slag, and 30% blast furnace slag (Shi 2004). Steel slag could be used in cement production in different ways: it can be used as raw material in the clinker production as was reported by Monshi and Asgarani (1999) and Tsakiridis et al. (2008), or can be blended in the cement as an mineral admixture (Xuequan et al. 1999; Rai et al. 2002; AkIn Altun and Yilmaz 2002; Kourounis et al. 2007) or aggregate, or just as a filler (Qasrawi et al. 2009; Sajkata et al. 2007).

In contrast to GGBS where the calcium and magnesium oxides combine and form non expansive compounds, in the metallurgical process of steel slag calcium and magnesium oxides are left free. Free lime expansion could occur due to the increase of volume caused by the hydration of lime to form calcium hydroxide. When steel slag is used in road construction it is a common practice to let it undergo a weathering process. This consists of leaving the slag in stockpiles exposed to the weather for a specific period of time in order to reduce its content of unhydrated lime.

Bin et al. (1992) reported a GGBS-steel slag cement which was alkali activated through the use of 5% of sodium silicate. In the same way, in a recent study Mahieux et al. (2009) conclude that weathered BOS slag seems to have little hydraulic activity

and apparently no pozzolanic properties; however, combining BOS slag with GGBS and small amounts of a catalyst (GGBS:52.5%, BOS:42.5%, catalyst:5%) gives very good results in terms of compressive strength. The activation of GGBS was attributed in part to the lime present in the BOS slag and in part due to the catalyst. In addition, it was found that the GGBS-BOS-catalyst cement did not presented expansion problems

The principal aim of the present work was to investigate the influence of steel slag and Portland cement on the evolution of the compressive strength and their effects on the hydration mechanisms of blended blast furnace slag pastes. For this, the mineralogical changes due to hydration, the setting times, the alkalinity of the raw materials and the pore solution, and the volume stability were measured on binary and ternary mixes.

## 2. Materials

The materials used in this research were obtained from different sources. A summary of them is presented below.

- A commercial **Ordinary Portland cement (OPC)** classified as CEM-1 according to British Standard BS EN 197-1 "*Composition, specifications and conformity criteria for common cements*".
- A **Ground Granulated blast furnace slag (GGBS)** obtained from Civil and Marine, a part of Hanson UK. The material was marketed under the standard BS 6699 "*Specification for ground granulated blast furnace slag for use with Portland cement*".
- A **Basic Oxygen slag (BOS)** obtained from Tarmac UK, from Corus Scuntorpe plant UK. It was ground and sieved through a 600 micron sieve before being used. Because the time between the grinding and use was more than one year, the slag is considered to be weathered.

Results for the composition of the oxides for all the materials are presented in table 1. The mineralogical composition of the materials was determined by X-ray diffraction Analysis (XRD) with a Philips 1820 diffractometer, and this was used for qualitative characterization of the materials. For normal OPC mineralogy, the principal phases have been widely studied and are well documented elsewhere (Chatterjee 2001). Figure 1 shows the phases  $C_3S$ ,  $C_2S$ ,  $C_3A$ , and  $C_4AF$  identified in the Portland cement used. In addition, there are some peaks that correspond to calcium carbonate (calcite). The mineral composition of the GGBS is shown in figure 2. As was reported by Taylor (1990), the XRD pattern for GGBS showed a diffuse band due to its amorphous high glassy and poor crystalline composition where merwinite and melilite were hardly differentiated.

The minerals associated with the basic oxygen slag are shown in figure 3. Although the patterns for this material shows peaks associated with calcium silicates ( $C_3S$  and  $C_2S$ ) these two phases in BOS slag are in insignificant quantity. According to Kourounis et al (2007) it is expected that the calcium silicates of the BOS would have been stabilized in the presence of impurities, reducing its cementitious properties. A common impurity found in the steel slag is metallic Fe; it was present in different forms as Wustite and Magnetite, compounds that have a negligible cementing capacity. The Portlandite phase ( $Ca(OH)_2$ ) was clearly observed, its presence is probably due to the weathering processes of the slag. It is suggested that the contact of the BOS with the environmental conditions of the laboratory hydrated the free lime producing calcium hydroxide and also carbonated some of it.

It is important to notice that the reactivity of the BOS slag depends on a combination of factors such as chemical and mineralogical composition, and fineness. In that way, a material with a completely defined crystal structure can be observed in figure 3 . From a qualitative point of view, it can be stated that the glass content of the BOS is negligible, so a slag with a minimal potential hydraulic reactivity is expected.

### **3. Laboratory testing program**

#### **3.1 Influence of the BOS and OPC on the compressive strength of GGBS mixtures**

In order to investigate the influence of the BOS and OPC on the strength of GGBS mixtures, an experimental laboratory programme was carried out. Paste mixes, (mixtures of the combination of one or more binders and water with no aggregate), with different proportions of ground granulated blast furnace slag, basic oxygen slag, and ordinary Portland cement were cast, cured and tested.

The OPC-GGBS-BOS ternary diagram in figure 4 shows the blends investigated with a total of 24 mixes. The location of the points represents the mixture proportions by weight. The selection of the mixes was made to cover the largest possible area inside the triangle. No aggregate was included because the principal aim was to assess the behaviour of the raw materials as binders, and the aggregate could introduce new parameters to study. The amount of water was kept constant for all mixes with a water binder ratio of 0.25.

For each mix 3 samples were cast in pre-oiled 50 mm cube moulds, covered with a polyethylene sheet and demoulded after 24 hours. Because of the differences among the raw materials and the proportions used, the mixes had different flow. In order to avoid affecting the compressive strength because of the differences in the mix compaction, all the mixes were compacted mechanically with a vibrating table. The moulds were filled with paste in three layers and compacted to remove the air and reach the maximum density. After demoulding the specimens were kept in containers at 98% RH and  $20 \pm 2$  °C.

The compressive strength was measured at 7, 28 and 90 days. A hydraulic testing machine was used in accordance with the ASTM C109: "*Compressive Strength of Hydraulic Cement Mortars*" (ASTM-C109).

### **3.2 Characterization of binders**

Several experiments were carried out in order to characterize and investigate the hydration mechanisms on selected GGBS blended binders (table 2). The initial setting times were determined by measuring the changes in their resistance to penetration by a standard needle with a Vicat apparatus (ASTM-C191 2008). For this

test the water binder ratio was equal to the normal consistency of each mix (ASTM-C187 2004).

The evolution of the initial temperature development of fresh paste samples was monitored introducing the samples into a semi-adiabatic container to quantify the temperature profile during the first 24 hours after mixing. The room where the tests were carried out had a controlled temperature of  $(20 \pm 2)$  °C. The samples were mixed according with the procedure presented above and were placed immediately inside the adiabatic chamber. The water binder ratio for all the mixes was 0.25 by weight.

A simple method was used to measure qualitatively the pH of the raw materials. For each material 100 g of powder and 50 g of distilled water were intensely mixed for 3 minutes until the mixture was completely homogeneous. After mixing, some 10 ml of suspension was poured into a test tube and the pH measured with a commercial pH meter electrode with resolution of 0.01 pH. It is important to notice that the pH measured does not correspond to the real pH developed for each final binder during the initial hydration. However, the pH comparison between all the raw materials can give some ideas about their potential alkalinity.

The pH of the pore fluid held within the pore structure of the paste of the binders was investigated a few hours after the mixing with an expression device similar to that described by Barneyback and Diamond (1981). Basically, a high tri-axial pressure (around 500 MPa) was applied to the paste in order to remould the pore distribution and express part of pore solution. Small cylinders were cast for each paste mix using plastic bottles of 50 mm diameter and 60 mm length. For all mixes the water binder ratio was of 0.25 and the tests were done 48 hours after casting. Around 10 ml of pore fluid was expressed from each sample and the pH was measured. The collected sample was titrated for pH as soon as possible to avoid carbonation.

The mineralogical composition developed due to the hydration process for different stages was determined by X-ray diffraction analysis (XRD) with the same equipment used to identify the cementitious powders. For this, samples with a water binder ratio of 0.25 were mixed and stored in small plastic bottles with tight lids to protect them from carbonation. The bottles were kept under controlled conditions of temperature

(20±2 °C) for 3, 28 and 90 days. For any desired age the sample was removed from the bottle, grounded to fineness less than the 200 mesh, and tested.

Finally, the length change for all final mixes was measured at early and later ages, determining their potential expansion or shrinkage. Standard moulds, according to ASTM C490 (1997) were used to cast prisms 25×25×285 mm for paste mixes with a water binder ratio of 0.25. A steel frame with an adjustable and a fixed anvil was used to hold the samples while the length was measured with a digital length gauge with a 0.001 mm scale.

## **4. RESULTS AND DISCUSSION**

### **4.1 Compressive strength of GGBS mixtures**

The influence of the combination of the raw materials on the compressive strength was analyzed. As each result corresponds to the average of three replicates, the variability of the experiments is shown with standard deviation error bars. Results of the average compressive strength of OPC-GGBS mixes are presented in figure 5. It can be seen that, for all ages, up to 60% GGBS replacement produces a slight reduction in the strength, while greater replacements have a more severe reduction in the strength. At 90 days there was an optimum value of GGBS replacement of 40% with a decrease of 6 percent in the strength. In the same way, the reduction of the strength measured at 90 days with a level of replacement of 60% was around 20%.

The results of average compressive strength at different ages for the combination of GGBS and BOS are presented in figure 6. It can be seen that the self-hydraulic properties of both materials are limited, especially for 100% BOS, which practically did not develop strength by itself after being hydrated. In the same way, the results for the mix of 100% GGBS shows that at 7 days there was low strength development (2 MPa), while at 28 days there was a slight increase of the strength (10 MPa). These results confirm that both slags need to be activated to develop their full hydraulic cementitious properties. In contrast, the combination of both slags showed



encouraging compressive strength results for low strength concrete applications. The optimum amount of BOS in mixes with both slags was equal to 40% and the strengths obtained at 7, 28 and 90 days were 10, 22, and 30 MPa respectively. That steady increment of strength shows a continuous hydration that can be presumably explained because of either the activation or reaction of the GGBS in the alkaline environment supplied by the steel slag.

Results of compressive strength for ternary OPC-GGBS-BOS mixes are presented in figure 7 for 7, 28 and 90 days. The nomenclature used was given according to the combinations of the materials. The mix O10G40B50 for example, means that there are 10% of OPC, 40% of GGBS and 50% of BOS. The compressive strength at 90 days for any combination of OPC, GGBS, and BOS is shown in figure 8 as iso-response or contour curves. In these figures, a new parameter called in this research slag index ( $I_s$ ) was proposed. This was defined as the amount of GGBS with respect the total amount of slag (1).

$$I_s = \frac{GGBS}{GGBS + BOS} \quad (1)$$

As was expected, for ternary mixes, the compressive strength increases as the percentage of OPC increases. In the same way, the behaviour of any compressive strength iso-line can be generalized by two lines: a “*line A*” defined by a straight line with a negative slope, where for the same strength a decrease in the amount of OPC corresponds to an increase in  $I_s$ , and a “*line B*” where an increase of the slag index has a limited effect on the compressive strength. In the figure a schematic representation of lines *A* and *B* has been included as dashed lines.

It is important to notice that the OPC is the most expensive of the materials, followed by the GGBS. In that way, the optimal mix will be one that includes a minimum of those materials. For any specific strength, this optimum corresponds to the intersection between lines *A* and *B* (point *C* in the figure). The point *C* changes its position depending on the iso-line value of strength selected and the age at which the compression test was conducted. It can be seen that the location of point *C* is at a slag index between 40 and 60% for most cases depending on the percentage of OPC used. An  $I_s$  of 50% is a good estimate.

## 4.2 Properties of slag mixtures

The setting times were measured for the four binders stated in the table 2. The change of the penetration depth during the first hours after mixing is shown in figure 9, where a period can be seen for all binders with practically no penetration resistance and a period where the penetration resistance increases linearly with time. There are significant differences in the rate of initial setting for samples with and without Portland cement; in OPC mixes the addition of any slag produces a relatively short delay in the start of setting. The mix OPC-GGBS showed an increase in the initial and final setting times of 18 and 41% respectively, and the mix OPC-GGBS-BOS showed an increase in the initial and final setting times of 30% and 50% respectively. All GGBS mixes activated with OPC had values of initial setting time in the range suggested by ASTM C150 (2007): >45 min and <375 min. In contrast, the mix GGBS-BOS showed a prolonged delay in the initial and final setting times, those were 293 and 315 % longer than the OPC sample.

The early age development of temperature measured in an adiabatic cell during the first 24 hours of hydration is shown in figure 10. Although the rate of temperature rise and the maximum temperatures were different for each binder, all samples had a similar profile: a sustained increase of the temperature until a maximum value was reached followed by a sustained temperature decreasing. It is important to notice that some slag samples had a secondary local maximum. In the OPC reference sample the temperature increased rapidly during the first 7 hours and reached a maximum increment of 25°C, after this time the sample started to reduce temperature until 22 hours when the temperature increase was negligible.

In the samples OPC-GGBS and OPC-GGBS-BOS in addition to the maximum peak, some local or secondary maximum points were measured. These local maximum peaks appeared a couple hours before the maximum peak and were followed in all cases by an inflection point. This behaviour reported by Roy and Idorn (1982) is characteristic of the early age hydration of GGBS, and Shy and Day (1995) state that the secondary peaks are the result of chemical reactions of the granulated slag and the alkalis used as activators. In the same way, De Schutter (1999) affirms that the reason for the presence of temperature multi-peaks can be explained by the fact that

the hydration of slag cements is due of two reactions: a Portland reaction and a slag-alkali reaction.

The temperature rise for mixes OPC-GGBS and OPC-GGBS-BOS was very similar. The maximum peak measured was around 12°C, however, in the ternary binder there was a delay of 2 hours approximately. At 24 hours for both samples there were remaining increments of temperature. The profile of the binder GGBS-BOS showed that by itself it is able to develop some exothermic reactions. The granulated slag is activated by the steel slag, and although the values obtained do not show strong reactions, it can be considerate by itself a poor hydraulic binder.

The results of pH for the raw materials are shown in figure 11-left. The pH depends on the concentration so the powders were all hydrated with a water binder ratio of 0.5, to obtain the differences in alkalinity. The GGBS, for example, showed the lowest value of alkalinity. According to Taylor (1990), this result can explain why if granulated slag is mixed alone with water it can develop just a small degree of hydration. As was stated before, a protective film deficient in  $\text{Ca}^+$  inhibits further reaction, but if the pH is kept sufficiently high the reaction continues. The lower basicity of GGBS compared with the Portland cement has been reported previously by Tailing and Krivenko (1997). In a research by Song and Jennings (1999), it was established that the pH of a mixing solution must be higher than 11.5 to activate the GGBS. They state that in a pH lower than 11.5 the solubility of silica is low and GGBS does not dissolve and form silicate hydrates as principal compounds. The pH of the Portland cement and steel slag is higher than the blast furnace slag, and presumably influenced their alkaline activation.

The pH of the pore solution of the final binders after 48 hours of hydration is shown in figure 11-right. Although the lime and metal alkali contents for OPC are considerably higher than for BOS (table 1), the pH of the extracted pore solution of the sample of OPC-GGBS-BOS was slightly higher than the OPC binder. This was because most of the lime in the BOS did not form any hydration compounds and remained partly free in the pore solution.

The development of the final binders with time determined by XRD is shown in figures 12 and 14. They show the X-ray pattern obtained after 3, 28 and 90 days of curing under controlled conditions of temperature and humidity. Although the principal crystalline hydration products were determined, it was not possible to observe the amorphous CSH gel by means of this technique.

The X-ray data for the 100% Portland cement reference (OPC), figure 12, shows a normal pattern which is discussed extensively in references books (Taylor 1990; Hewlett 1988). Calcium hydroxide, known as portlandite (CH), was formed in significant quantities from the early ages as the result of the hydration of calcium silicates. This compound remained stable throughout the period of investigation. Calcite or calcium carbonate (CC) was present, probably due to small amounts of limestone in the Portland cement. During the mixing and curing the contact of the samples with carbon dioxide was limited, although during the x-ray preparation of the samples or even during the x-ray scanning there could have been some minor carbonation. It is believed that the carbonation, if present, was minimal and is not responsible for the presence of calcium carbonate. The peak found at  $29.4^{\circ}2\theta$  overlaps the calcite and the  $C_3S$  or alite ( $C_3$ ), however it decreases during curing meaning that some cement compounds had a hydration delay. At three days, there were some un-hydrated calcium silicates ( $C_3$ ,  $C_2$ ). They decrease in intensity during curing, but at 90 day there were some remaining. As was expected, ettringite (E) was present as a stable compound.

The X ray traces for the 40% Portland cement and 60% blast furnace slag mix are shown also in figure 12. The system had similar hydration products to Portland cement; however, the intensity of portlandite was lower because a smaller amount of OPC was used. It can be noted that during all the period studied there are no differences in the amount of calcium hydroxide and it remains constant. From this observation, it is shown that during the hydration of GGBS in a Portland cement system the slag does not consume the calcium hydroxide available. The alkalis released from Portland cement are responsible for activating the slag as is shown in the model of figure 13 (Roy and Idorn (1982). Other minerals found in the pattern were calcite, anhydrous calcium silicates and ettringite.

The X ray pattern for the 60%GGBS+40%BOS mix is shown in figure 14. This mix does not have any Portland cement addition and is made up entirely of slag. It is important to notice that from the X-ray pattern there is not evidence of the presence of calcium hydroxide. This compound was abundant in the non-hydrated steel slag, but is not present in the hydrated binary slag mix. The absence of portlandite can be explained qualitatively in figure 13-right where the proposed mechanism of hydration for the GGBS-BOS mix is shown. This consists of the consumption of the calcium hydroxide supplied by the BOS in reactions of GGBS before 3 days of hydration, producing some sort of calcium silicate hydrates (C- $\gamma$ -S-H). Although this C- $\gamma$ -S-H gel sets and develops some strength, it is much weaker than that obtained from the slag reaction with OPC. It is believed that this mechanism of hydration can occur principally in non-Portland mixes.

The pattern for the ternary 40%OPC+30%GGBS+30%BOS mix is shown also in figure 14. It can be seen that the peaks follow the pattern left by the cement hydration and similar minerals were obtained. For this mix, the mechanisms of hydration can be summarized as follows: the hydration of the OPC by itself and the hydration of the slag through the alkalis available. In this ternary mix there is no evidence of calcium hydroxide consumption, according to the X-ray diffraction patterns the lime increased with time.

The length change of samples was measured for OPC, OPC-GGBS, and OPC-GGBS-BOS at different days and results are reported as percentage at different ages in figure 15. No considerable expansion or shrinkage was measured for any of the mixes; all the ranges are smaller than 0.05% and are relatively stable in time. No expansion was measured in the mix containing BOS, in contrast with the reported in the literature. The dimensional stability of the mix containing BOS is attributed to the weathered condition of the steel slag and the compensation due to the trend of the GGBS to have some shrinkage.

## 5. Conclusions

The main conclusions may be drawn from the above findings are:

1. The influence of the replacement level of ordinary Portland cement and steel slag on the compressive strength of ground granulated blast furnace slag blended binders has been studied in detail. A proposed parameter called “slag index” has been introduced and the optimal value found was 0.5 in samples with OPC.
2. The steel slag used in this research can be used as activator for GGBS. The material, weathered naturally under laboratory conditions, can be used effectively in ternary mixes composed of OPC-GGBS-BOS.
3. No expansion was measured in the mixes tested; it gives encouraging results for the potential use of blended mixes of weathered steel and blast furnace slag.

#### 4. REFERENCES

- ACI-233 (2003) 233R-03: Slag Cement in Concrete and Mortar. *ACI - American Concrete Institute*.
- AKIN ALTUN, I. & YILMAZ, I. (2002) Study on steel furnace slags with high MgO as additive in Portland cement. *Cement and Concrete Research*, 32, 1247-1249.
- ASTM-C109 Standard Test Method for Compressive Strength of Hydraulic Cement Mortars (Using 2-in. or [50-mm] Cube Specimens).
- ASTM-C150 (2007) Standard Specification for Portland Cement.
- ASTM-C187 (2004) Standard Test Method for Normal Consistency of Hydraulic Cement.
- ASTM-C191 (2008) Standard Test Methods for Time of Setting of Hydraulic Cement by Vicat Needle.
- ASTM-C490 (1997) Standard Practice for Use of Apparatus for the Determination of Length Change of Hardened Cement Paste, Mortar, and Concrete
- ASTM-C595 (2008) Standard Specification for Blended Hydraulic Cements.
- BARNEYBACK JR, R. S. & DIAMOND, S. (1981) Expression and analysis of pore fluids from hardened cement pastes and mortars. *Cement and Concrete Research*, 11, 279-285.
- BIN, Q., WU, X. & TANG, M. (1992) High strength alkali steel-iron slag binder. *Proc., 9th Int. Congress on the Chemistry of Cement*. New Delhi, India.
- CHATTERJEE, A. K. (2001) X-Ray Diffraction. IN RAMACHANDRAN, V. S. & BEAUDOIN, J. J. (Eds.) *Handbook of Analytical Techniques in Concrete Science and Technology*. NOYES PUBLICATIONS.
- DE SCHUTTER, G. (1999) Hydration and temperature development of concrete made with blast-furnace slag cement. *Cement and Concrete Research*, 29, 143-149.
- DETWILER, R., BHATTY, J. & BHATTACHARJA, S. (1996) *Supplementary Cementing Materials for Use in Blended Cements* PCA-RD112.
- GEISELER, J. (1996) Use of steelworks slag in Europe. *Waste Management*, 16, 59-63.

- HEWLETT, P. (1988) *Lea's Chemistry of Cement and Concrete*.
- KOUROUNIS, S., TSIVILIS, S., TSAKIRIDIS, P. E., PAPADIMITRIOU, G. D. & TSIBOUKI, Z. (2007) Properties and hydration of blended cements with steelmaking slag. *Cement and Concrete Research*, 37, 815-822.
- MAHIEUX, P. Y., AUBERT, J. E. & ESCADEILLAS, G. (2009) Utilization of weathered basic oxygen furnace slag in the production of hydraulic road binders. *Construction and Building Materials*, 23, 742-747.
- MATSCHEI, T., BELLMANN, F. & STARK, J. (2005) Hydration behaviour of sulphate-activated slag cements. *Advances in Cement Research*, 17.
- MONSHI, A. & ASGARANI, M. K. (1999) Producing Portland cement from iron and steel slags and limestone. *Cement and Concrete Research*, 29, 1373-1377.
- QASRAWI, H., SHALABI, F. & ASI, I. (2009) Use of low CaO unprocessed steel slag in concrete as fine aggregate. *Construction and Building Materials*, 23, 1118-1125.
- RAI, A., PRABAKAR, J., RAJU, C. B. & MORCHALLE, R. K. (2002) Metallurgical slag as a component in blended cement. *Construction and Building Materials*, 16, 489-494.
- ROY, D. M. & LDORN, G. M. (1982) Hydration, Structure, and Properties of Blast Furnace Slag Cements, Mortars, and Concrete. *ACI -Journal Proceedings*, 79.
- SAJKATA, AYANO & FUJII (2007) Steel making slag concrete as sustainable construction materials. *Sustainable construction materials and technologies* Coventry, UK.
- SHI, C. (2004) Steel Slag—Its Production, Processing, Characteristics, and Cementitious Properties. *J. Mat. in Civ. Engrg*, 16, 230-236
- SHI, C. & DAY, R. L. (1995) A calorimetric study of early hydration of alkali-slag cements. *Cement and Concrete Research*, 25, 1333-1346.
- SONG, S. & JENNINGS, H. M. (1999) Pore solution chemistry of alkali-activated ground granulated blast-furnace slag. *Cement and Concrete Research*, 29, 159-170.
- TAILING, B. & KRIVENKO, P. (1997) Blast Furnace Slag – The Ultimate Binder. IN CHANDRA, S. (Ed.) *Waste Materials used in Concrete Manufacturing*.
- TAYLOR, H. F. W. (1990) *Cement Chemistry*, Academic Press.
- TSAKIRIDIS, P. E., PAPADIMITRIOU, G. D., TSIVILIS, S. & KORONEOS, C. (2008) Utilization of steel slag for Portland cement clinker production. *Journal of Hazardous Materials*, 152, 805-811.
- XUEQUAN, W., HONG, Z., XINKAI, H. & HUSEN, L. (1999) Study on steel slag and fly ash composite Portland cement. *Cement and Concrete Research*, 29, 1103-1106.

Binder	Specific	Chemical composition [%]											
	Gravity	SiO <sub>2</sub>	TiO <sub>2</sub>	Al <sub>2</sub> O <sub>3</sub>	Fe <sub>2</sub> O <sub>3</sub>	MnO	MgO	CaO	Na <sub>2</sub> O	K <sub>2</sub> O	P <sub>2</sub> O <sub>5</sub>	SO <sub>3</sub>	LOI
OPC*	3.11	19.7	---	4.9	2.4	---	2.1	63.3	0.2	0.6	---	2.7	2.7
GGBS	2.94	34.5	0.55	13.16	0.74	0.45	7.75	38.7	0.29	0.55	0.02	1.75	0.7
BOS	3.49	11.45	0.37	2.32	27.32	3.65	9.32	37.44	0.03	0.01	1.26	0.28	3.12

Table 1 Chemical oxide composition (\*according to the producer)

Binder	Materials	Binder name
1	100% OPC (reference)	OPC
2	40% OPC + 60% GGBS	OPC-GGBS
3	40% OPC + 30% GGBS + 30% BOS	OPC-GGBS-BOS
4	60%GGBS+40%BOS	GGBS-BOS

Table 2 Final mixes tested

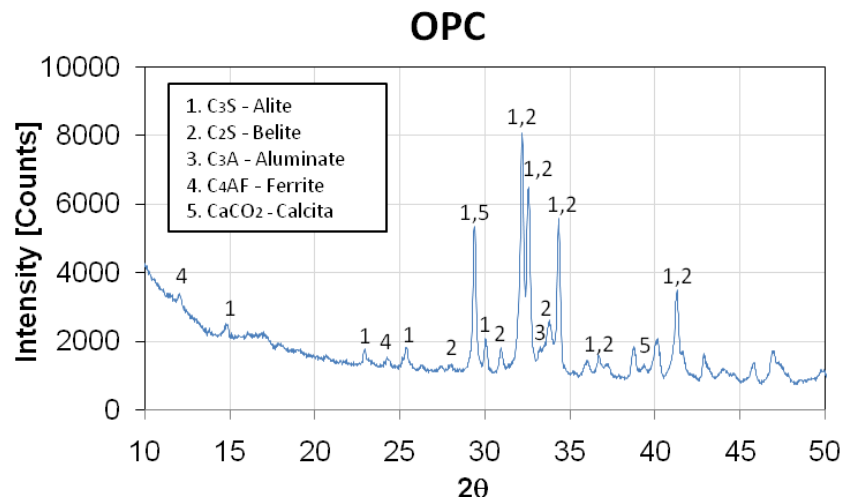


Figure 1 XRD analyses of OPC

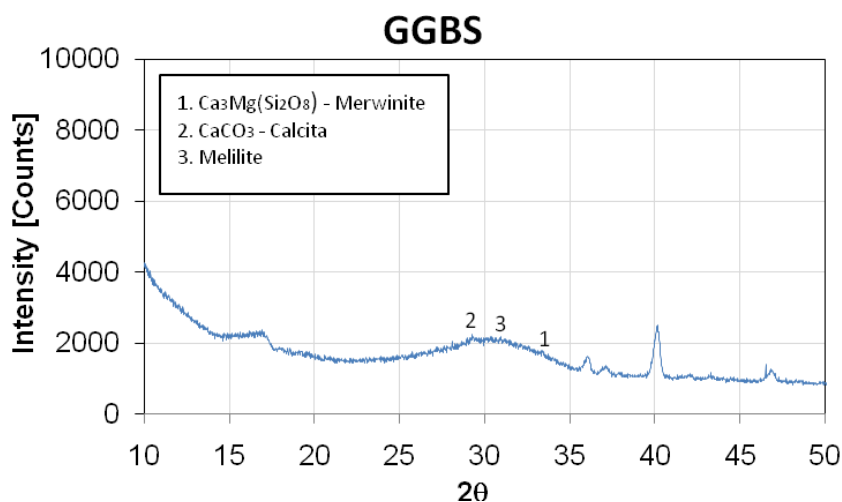


Figure 2 XRD analyses of GGBS



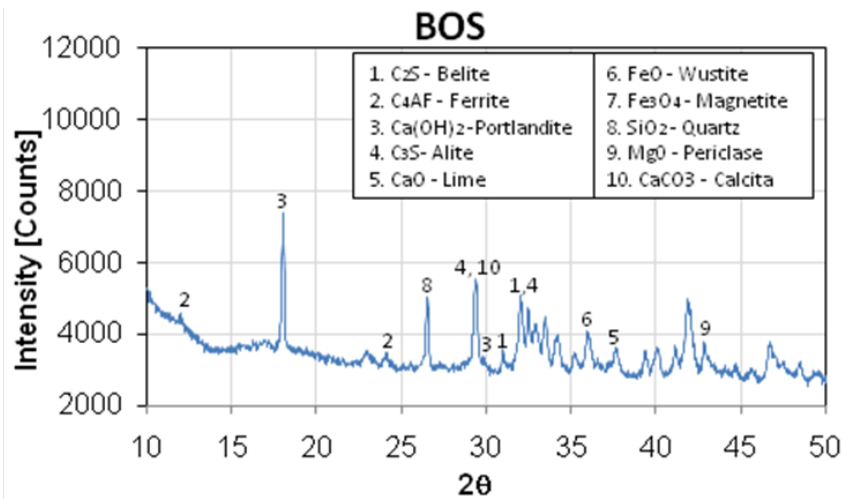


Figure 3 XRD analyses of BOS

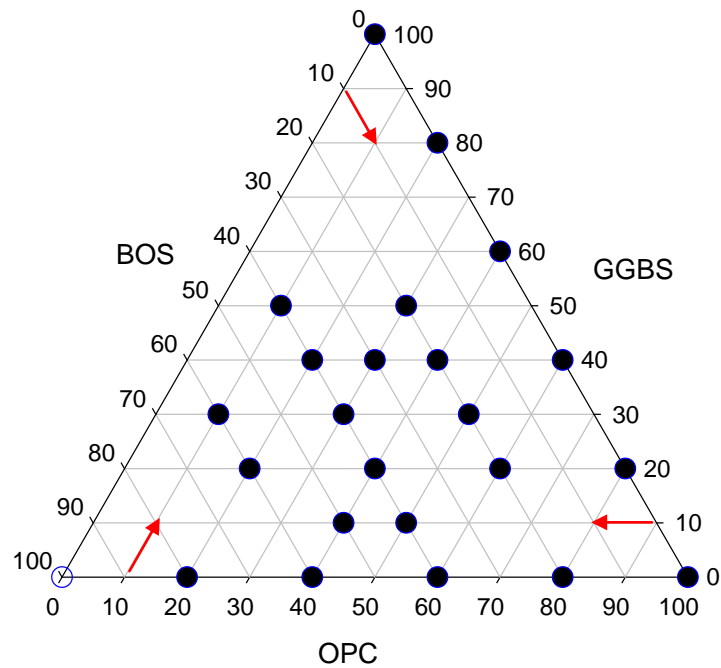


Figure 4 Compressive strength mixtures tested

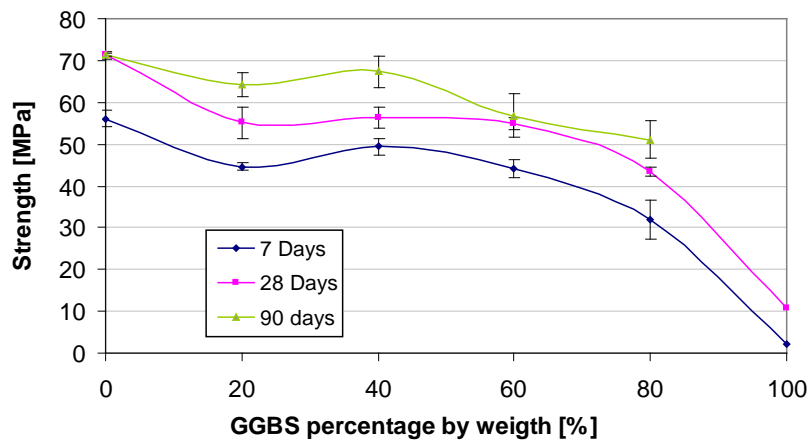


Figure 5 Compressive strength of OPC-GGBS mixes

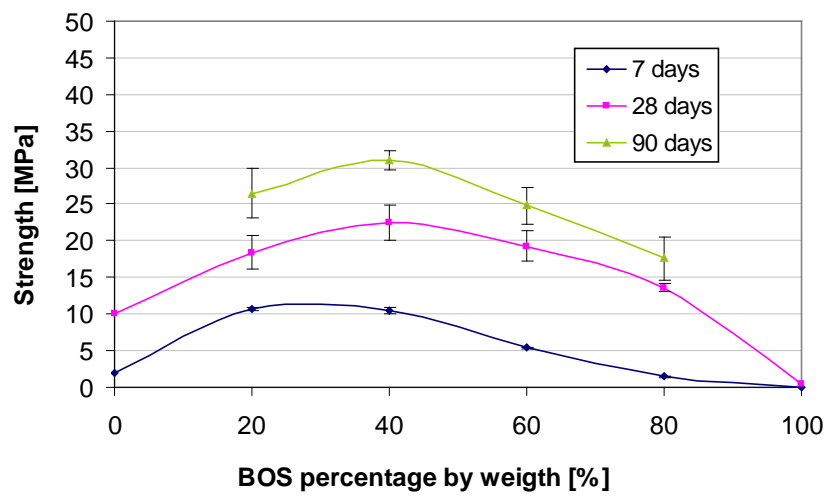


Figure 6 Compressive strength of BOS-GGBS mixes

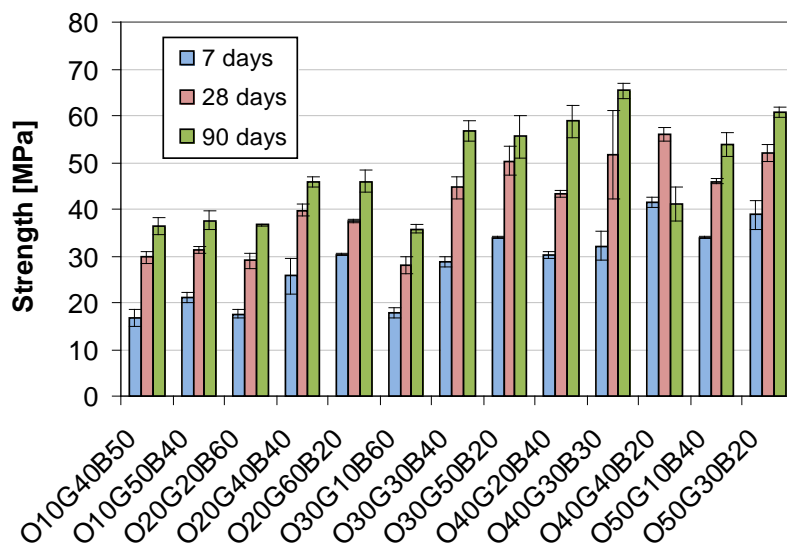


Figure 7 Compressive strength ternary mixes OPC-GGBS-BOS

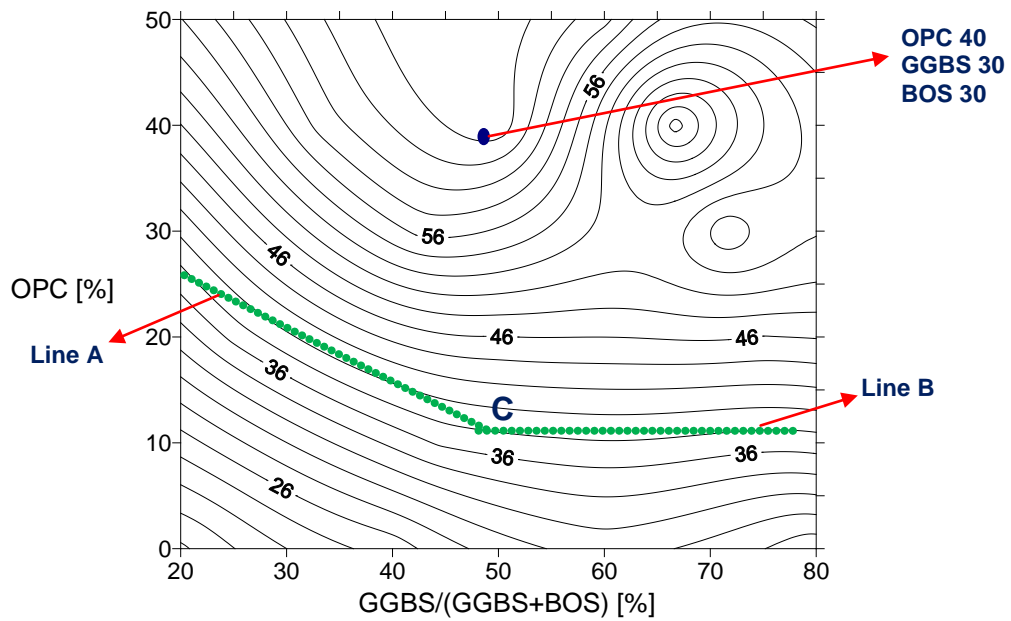


Figure 8 Compressive strength 90 days

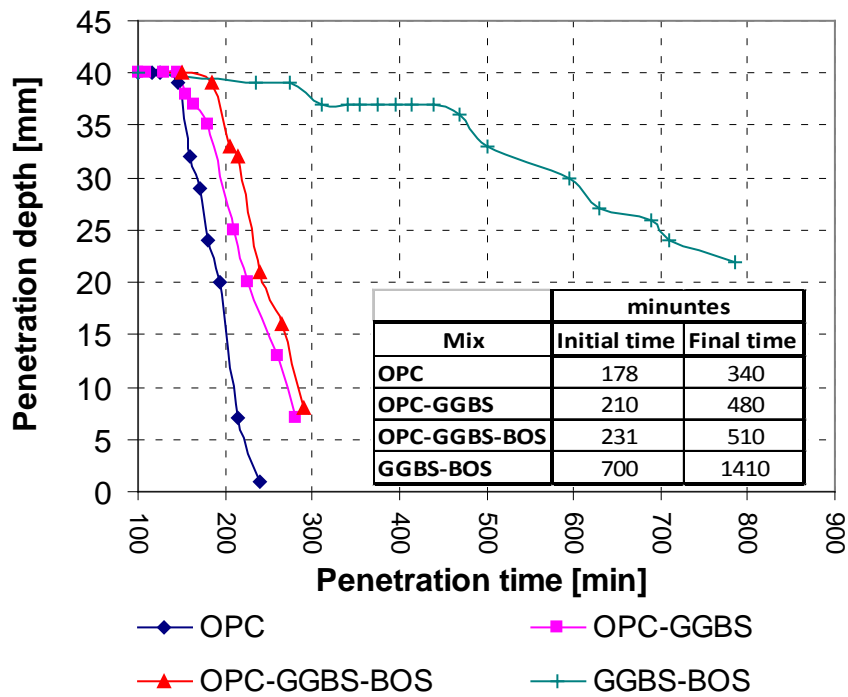


Figure 9 Vicat needle Penetration and Setting times

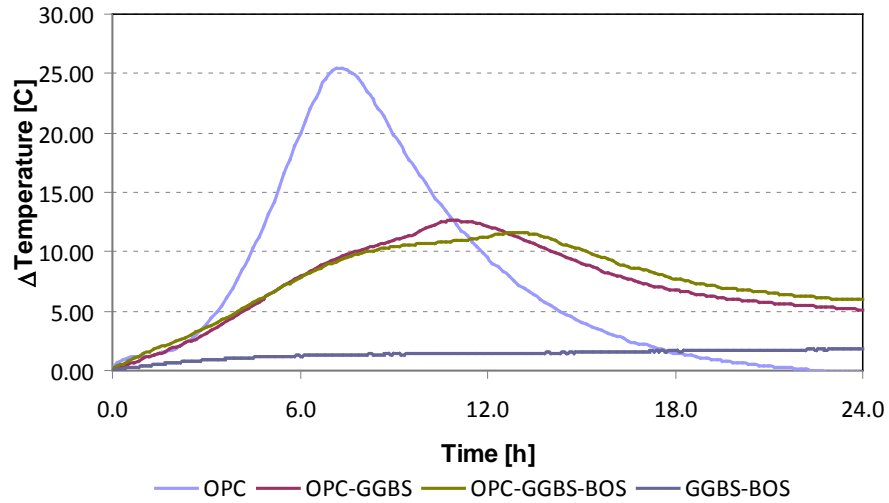


Figure 10 temperature rise of blended GGBS mixes

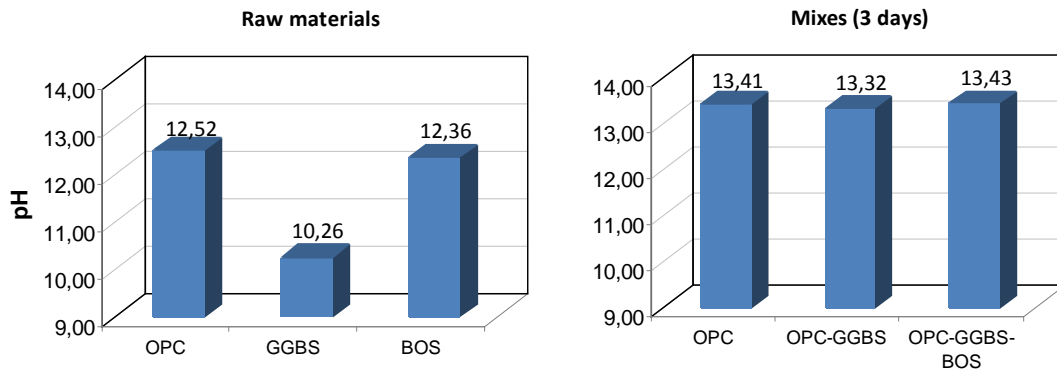


Figure 11 pH of the raw materials and pH of the pore solutions of the final binders after 3 days of casting

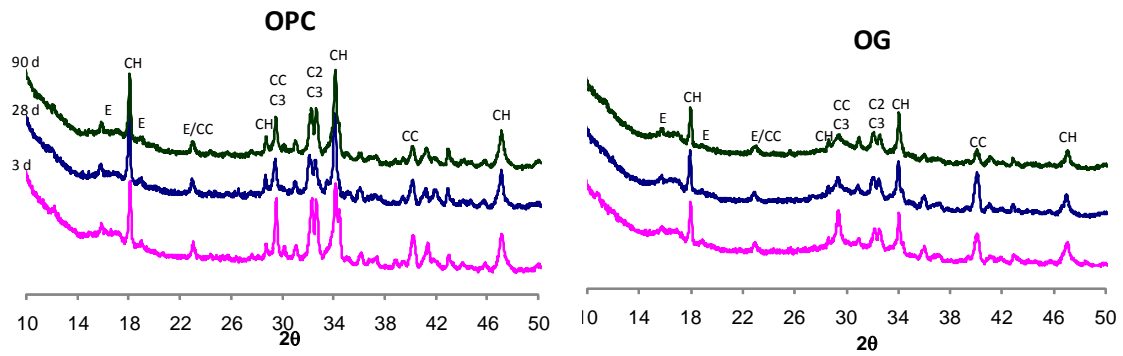


Figure 12 X-ray pattern of OPC and OPC-GGBS (OG) mixes for different ages

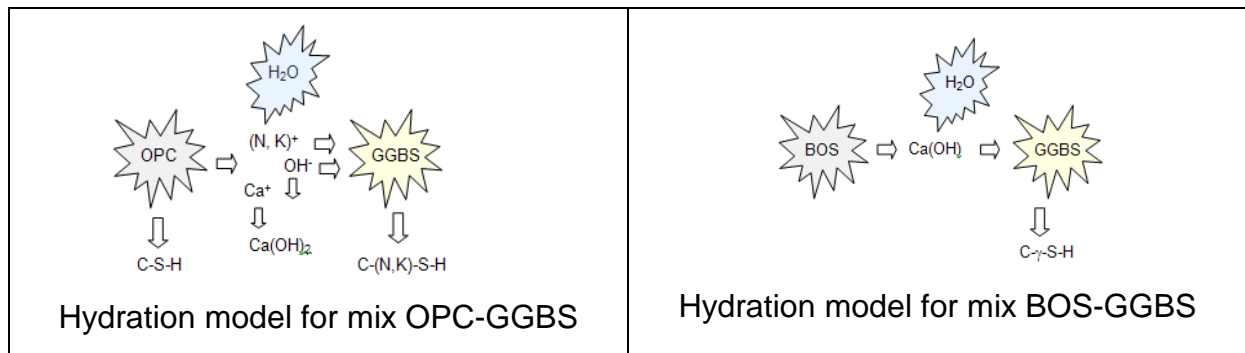


Figure 13 GGBS Hydration models

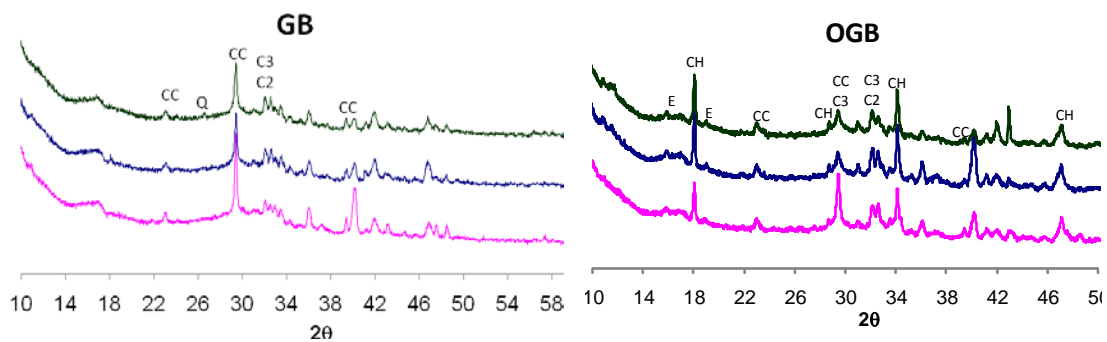


Figure 14 X-ray pattern of the GGBS-BOS (GB) and OPC-GGBS-BOS (OGB) mixes for different ages

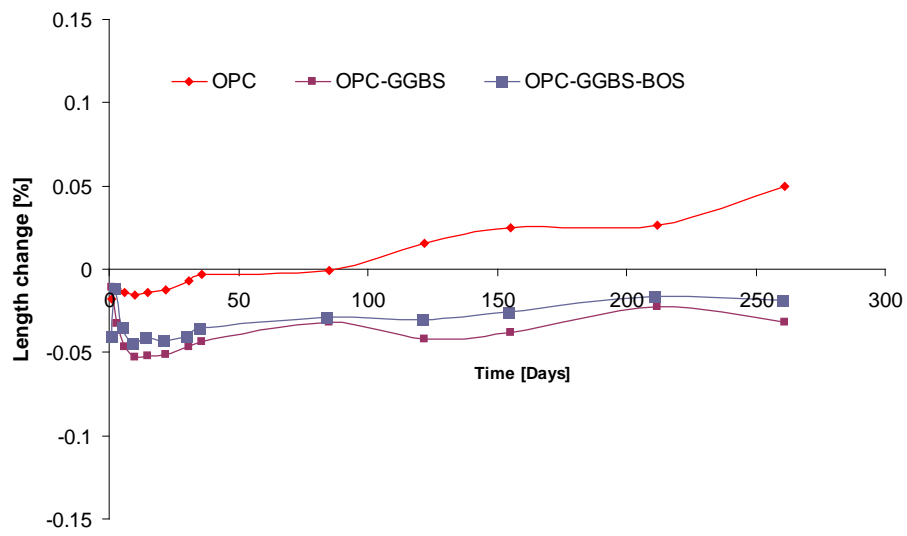


Figure 15 Volume stability of GGBS mixes